REPORT DOCUMENTATION PAGE

Form Approved OMB NO. 0704-0188

1. REPORT DATE (DD-MM-YYYY)	2. REPORT TYPE	3. DATES COVERED (From - To)
31-10-2014	Final Report	1-Aug-2013 - 31-Jul-2014

4. TITLE AND SUBTITLE
Final Report: Fast Ultrasound System for Imaging and Probing the Dynamic Response of Granular Materials

5a. CONTRACT NUMBER
W911NF-13-1-0330

5b. GRANT NUMBER

5c. PROGRAM ELEMENT NUMBER
611103

6. AUTHORS
Heinrich Jaeger

5d. PROJECT NUMBER

5e. TASK NUMBER

5f. WORK UNIT NUMBER

7. PERFORMING ORGANIZATION NAMES AND ADDRESSES
University of Chicago
5801 South Ellis Avenue

Chicago, IL 60637 -5418

8. PERFORMING ORGANIZATION REPORT NUMBER

9. SPONSORING/MONITORING AGENCY NAME(S) AND ADDRESS (ES)
U.S. Army Research Office
P.O. Box 12211
Research Triangle Park, NC 27709-2211

10. SPONSOR/MONITOR'S ACRONYM(S)
ARO

11. SPONSOR/MONITOR'S REPORT NUMBER(S)
63464-MS-RIP.1

12. DISTRIBUTION AVAILIBILITY STATEMENT
Approved for Public Release; Distribution Unlimited

13. SUPPLEMENTARY NOTES
The views, opinions and/or findings contained in this report are those of the author(s) and should not contrued as an official Department of the Army position, policy or decision, unless so designated by other documentation.

14. ABSTRACT
Granular materials are random aggregates of a large number of macroscopic, individually solid particles that interact primarily via dissipative contacts among neighboring grains. They exhibit complex dynamics in which the aggregate can transition between solid?like “jammed” and liquid-like “unjammed” behavior. Connecting local, particle-scale properties to the overall, aggregate response when large stresses are applied is of fundamental interest for developing accurate models for the onset (or demise) of aggregate rigidity. It also provides a path toward engineering new classes of particulate materials with aggregate responses “by design”. This project established new

15. SUBJECT TERMS
ultrasound, imaging, non-Newtonian, shear flow

16. SECURITY CLASSIFICATION OF:			17. LIMITATION OF ABSTRACT	15. NUMBER OF PAGES	19a. NAME OF RESPONSIBLE PERSON
a. REPORT	b. ABSTRACT	c. THIS PAGE			Heinrich Jaeger
UU	UU	UU	UU		19b. TELEPHONE NUMBER 773-702-6074

Report Title

Final Report: Fast Ultrasound System for Imaging and Probing the Dynamic Response of Granular Materials

ABSTRACT

Granular materials are random aggregates of a large number of macroscopic, individually solid particles that interact primarily via dissipative contacts among neighboring grains. They exhibit complex dynamics in which the aggregate can transition between solid?like "jammed" and liquid-like "unjammed" behavior. Connecting local, particle-scale properties to the overall, aggregate response when large stresses are applied is of fundamental interest for developing accurate models for the onset (or demise) of aggregate rigidity. It also provides a path toward engineering new classes of particulate materials with aggregate responses "by design". This project established new research capabilities high-speed, non-invasive ultrasound imaging of particle configurations during jamming and unjamming events. An advanced ultrasound imaging system was set up and calibrated for imaging of fast jamming processes in dense suspensions of non-Brownian particles, such as propagating density fronts, where both high temporal and spatial resolution is required. The ultrasound imaging system is comprised of hardware components for shaping, transmitting and receiving ultrasound signals in the frequency range 1-15MHz and can achieve acquisition rates up to 10,000 full image frames per second.

Enter List of papers submitted or published that acknowledge ARO support from the start of the project to the date of this printing. List the papers, including journal references, in the following categories:

(a) Papers published in peer-reviewed journals (N/A for none)

Received Paper

TOTAL:

Number of Papers published in peer-reviewed journals:

(b) Papers published in non-peer-reviewed journals (N/A for none)

Received Paper

TOTAL:

Number of Papers published in non peer-reviewed journals:

(c) Presentations

Number of Presentations: 0.00

Non Peer-Reviewed Conference Proceeding publications (other than abstracts):

Received Paper

TOTAL:

Number of Non Peer-Reviewed Conference Proceeding publications (other than abstracts):

Peer-Reviewed Conference Proceeding publications (other than abstracts):

Received Paper

TOTAL:

Number of Peer-Reviewed Conference Proceeding publications (other than abstracts):

(d) Manuscripts

Received Paper

TOTAL:

Number of Manuscripts:

Books

Received Book

TOTAL:

Received	Book Chapter

TOTAL:

Patents Submitted

Patents Awarded

Awards

Graduate Students

NAME	PERCENT_SUPPORTED	Discipline
Endao Han	0.00	
FTE Equivalent:	**0.00**	
Total Number:	**1**	

Names of Post Doctorates

NAME	PERCENT_SUPPORTED
Ivo Peters	0.00
FTE Equivalent:	**0.00**
Total Number:	**1**

Names of Faculty Supported

NAME	PERCENT_SUPPORTED	National Academy Member
Heinrich Jaeger	0.00	
FTE Equivalent:	**0.00**	
Total Number:	**1**	

Names of Under Graduate students supported

NAME	PERCENT_SUPPORTED
FTE Equivalent:	
Total Number:	

Student Metrics

This section only applies to graduating undergraduates supported by this agreement in this reporting period

The number of undergraduates funded by this agreement who graduated during this period: 0.00

The number of undergraduates funded by this agreement who graduated during this period with a degree in science, mathematics, engineering, or technology fields:..... 0.00

The number of undergraduates funded by your agreement who graduated during this period and will continue to pursue a graduate or Ph.D. degree in science, mathematics, engineering, or technology fields:..... 0.00

Number of graduating undergraduates who achieved a 3.5 GPA to 4.0 (4.0 max scale):..... 0.00

Number of graduating undergraduates funded by a DoD funded Center of Excellence grant for Education, Research and Engineering:..... 0.00

The number of undergraduates funded by your agreement who graduated during this period and intend to work for the Department of Defense 0.00

The number of undergraduates funded by your agreement who graduated during this period and will receive scholarships or fellowships for further studies in science, mathematics, engineering or technology fields: 0.00

Names of Personnel receiving masters degrees

NAME

Total Number:

Names of personnel receiving PHDs

NAME

Total Number:

Names of other research staff

NAME	PERCENT_SUPPORTED

FTE Equivalent:

Total Number:

Sub Contractors (DD882)

Inventions (DD882)

Scientific Progress

see attachment

Technology Transfer

Contract Number: W911NF-13-1-0330

Fast Ultrasound System for Imaging and Probing the Dynamic Response of Granular Materials

PI: Heinrich Jaeger, University of Chicago

Final Progress Report

August 01, 2013 to July 31, 2014

Table of Contents

Scientific Progress and Accomplishments

Statement of the Problem Studied

Granular materials are random aggregates of a large number of macroscopic, individually solid particles that interact primarily via dissipative contacts among neighboring grains. They encompass a wide range of technologically relevant particulate media from sand, gravel, or soil to agricultural products like grain or fertilizer to pharmaceutical powders. Many of the non-liquid raw ingredients used for processing in industry come in granular form, for example during cement production or for casting and making moulds. Foundations, gravel beds for railroad ties, levies and harbor jetties all depend for optimal performance on the careful choice of particles that comprise the granular aggregate.

A detailed understanding of the dynamics of granular materials is of importance to the US Army's mission on many levels. The fact that these materials, in aggregate, differ from ordinary solids and liquids is at once the basis for their uses as dams, road beds or impact energy dissipating structures, but also a source of an astoundingly complex dynamics in which the aggregate can transition between solid-like "jammed" and liquid-like "unjammed" behavior. In addition, there is highly dissipative plastic deformation of the particle arrangement during any type of impact or when stress is applied, for example by wheeled vehicles. From a basic scientific perspective granular matter provides a paradigm for emergent cooperative behavior in a nonlinear and dissipative system far from equilibrium.

In order to investigate jamming and unjamming transitions in granular materials and dense suspensions, a two key issues are the opaqueness of the material and the need for high speed imaging to capture important transient behavior. X-ray imaging is a possibility, but requires special high-intensity equipment to reach high frame rates. Ultrasound is also suitable for opaque media, but traditional ultrasound imaging systems are relatively slow, because they build up an image by line scanning. Given that the speed of sound puts a hard limit on the time to measure a single line, typical frame rates have been limited to 30 fps. However, recent developments in ultrasound imaging have made it possible to reconstruct images using a single pulse and have pushed the frame rate up to around 10,000 fps.

The project goal was to set up a high-speed ultrasound system specifically optimized to image complex non-Newtonian flows near the onset of jamming in dense suspensions. The rapid, non-invasive access to flow fields and particle reconfigurations from the interior of the suspension enables completely new possibilities to study the connection between local, particle-level and overall aggregate response to shear and impact near the jamming transition.

Summary of the Results

Below we describe the progress since the Verasonic fast ultrasound imaging system was purchased and installed. The following sections describe the set-ups that we have built to integrate the ultrasound system with our experiments that investigate the jamming transition, the calibrations we have performed, and the first data we have obtained with the fast ultrasound imaging system.

Set-up and Calibration

One of the main advantages of the ultrasound system is to complement apparatuses that measure forces with visualization of the sample. We have therefore designed set-ups that integrate the Verasonics system with the following three systems:

(i) Instron materials tester, for slow, but highly controlled compressional and extensional forcing. Speeds go up to 8 mm/s, forces up to 50 kN.
(ii) Linear actuator, for fast forcing by compression or extension, up to 400 mm/s. Achievable forces up to ~100 N.
(iii) Anton Paar rheometer, for controlled rotational measurements. High precision torque measurements (accuracy 10^{-9} Nm).

Besides integrating these systems for use with ultrasound, we also performed general calibration measurements for the suspensions that we use. These calibrations include determining basic properties like the speed of sound and attenuation coefficients.

Instron and Linear Actuator

Both the Instron materials tester and the linear actuator apply linear motion, with the main difference of concern the speed of the motion and the accuracy of measured force and displacement. The procedure for integration with ultrasound imaging therefore is similar, and we only show the setup for the Instron / Verasonics combination. A photo and a schematic of the setup are shown in Figure 1. The purpose of the set-up is to observe the motion of objects, such as the reflector, within the sample and the motion of the sample itself through an ultrasound transducer placed beneath the bottom of the sample.

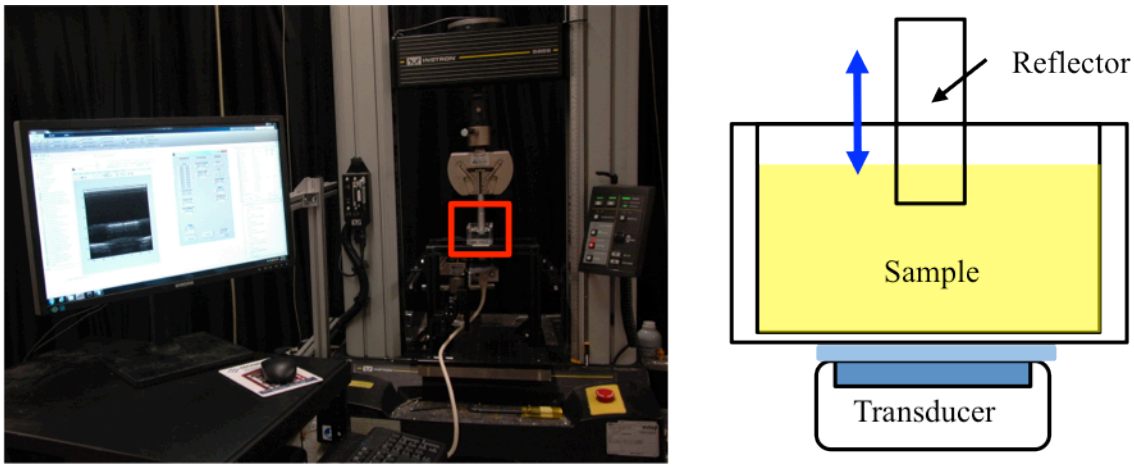

Figure 1 – Left: Photo of the setup, showing part of the ultrasound system and how it is combined with the Instron material tester. Right: Schematic view of the setup in the red box where the reflector is attached to the Instron.

The sample, which could be either liquid or suspension, is placed in a container made of acrylic, polyethylene or thin plastic membranes depending on situations. Plastic membranes have the best acoustic properties, but in experiments involving impact or high pressure we need materials with enough stiffness to protect the transducer. The container rests on a platform with some space to put the transducer. Between the bottom of the container and the head of the transducer

we place a thin layer of ultrasound gel to get a better acoustic coupling. An bracket holds the transducer so that it can be translated along the X, Y, and Z directions and rotated along one axis. On top of the container is a reflector/pusher tool attached to the Instron (or linear actuator). The reflector can move vertically with computer-controlled position and velocity, and the force applied on the reflector is measured by the Instron as well. Though termed reflector, its functions are not limited to reflecting the sound wave back to the transducer. For example, in the experiments to visualize the propagation of the jamming front in cornstarch suspensions (see below), it impacts the surface of the suspension and the force response is measured simultaneously.

Rheometry

The set-ups described above are focused on the response to a compressive force. The following set-up is designed to investigate the behavior of suspensions under shear. It combines the Verasonics ultrasound imaging system with an Anton Paar rheometer. The measurement cell is based on a standard Couette geometry, which consists of two concentric cylinders: one outer fixed cylinder and a rotating the inner cylinder. The rheometer measures the applied torque on the inner cylinder, from which the properties of the sample can be calculated under several assumptions about the flow profile in the sample. Depending on the sample properties and measuring conditions, these assumptions are typically for steady state and are assumed to be homogeneous throughout the sample. Due to the highly nonlinear and unsteady response of the dense suspensions of this study, these assumptions cannot be made and visualization of the flow field is necessary.

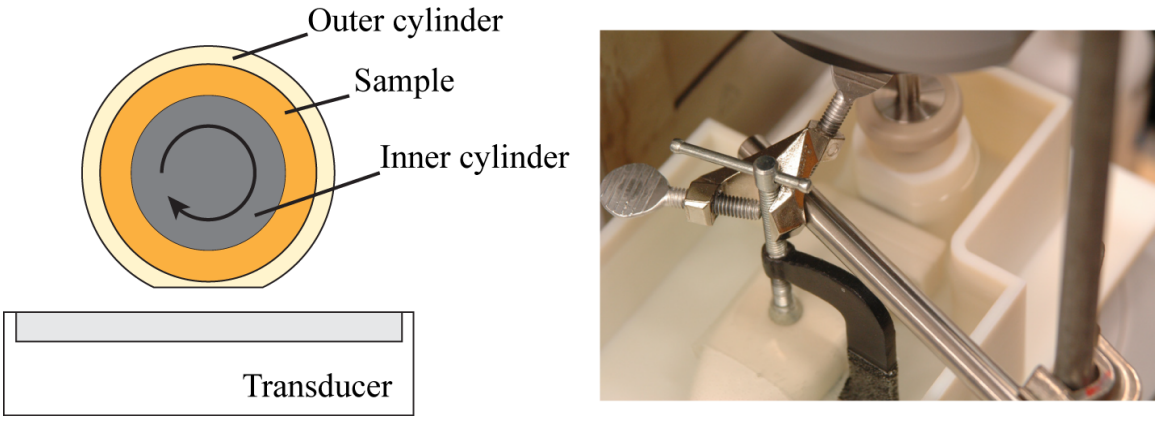

Figure 2 – Left: Schematic view of the setup where we combine ultrasound imaging with rheometry. Right: Photo of the setup, showing part of the outer container in which the transducer is submerged.

An outer cylinder in a typical Couette cell used with a rheometer is made of stainless steel. This is unsuitable for coupling ultrasound into the sample because of the large difference in acoustic impedance between water and steel. We have replaced the outer cylinder by a 3D-printed version, made from UV-cured polymer, which provides an excellent acoustic match to water. A schematic view of the transducer, outer, and inner cylinder is shown in Figure 2. The outer cylinder is connected to a larger water container, in which the transducer is submerged to optimize coupling into the sample. The acoustical path can now be described as follows: From the transducer into water, through the outer cylinder into the sample, reflection on the inner

cylinder, back through the sample, outer cylinder, water, and ending at the transducer. Distortion of the signal by the outer cylinder is further reduced, by making the outer wall flat at the side of the transducer. The outer cylinder, water container and base plate is 3D-printed as a single piece, with mounting points for the rheometer, to ensure accurate alignment with the rotating inner cylinder.

The photo (Figure 2, right) shows the 3D-printed measurement cell with the outer cylinder and the surrounding container, and the transducer being submerged in water. Not visible is the rheometer, except for a part of the tool that is inserted in the outer cylinder.

Calibration

The basic mechanism of the ultrasound system is to send out a pulse, such as the one illustrated in Figure 3, and measure the time it takes for it to be reflected back. Combined with the knowledge of the speed of sound in the medium we can calculate the distance between the transducer and the object that reflected the signal. Additionally, since the transducers have multiple (128 or 256) channels that transmit and receive signals, we can reconstruct a two-dimensional image of the medium we are studying based on the delay time and amplitudes of the reflected signals in all channels. Corresponding to this idea, we calibrated the ultrasound system in the following steps:

(i) Measure signals reflected back from a flat reflector in water to check the validity of time measurement, thus distance measurement.
(ii) Measure the attenuation of the signal in cornstarch suspension in order to improve the imaging quality.
(iii) Track the motion of scatters embedded in a continuous medium (gelatin) to check the validity of velocity field measurement in two dimensions.

Calibration for Water

Water provides a good initial test because (1) the acoustic properties are well known both theoretically and experimentally, and (2) the attenuation of sound in water is very weak which makes it easier to image large distances into the systems. In this case the sample used deionized water and the reflector was connected to the Instron so that its position could be controlled with precision. The transmitted pulse is an amplitude-manipulated wave as shown in Figure 3 (left) by the red curve. In this case the pulse consisted of a 5MHz sinusoidal wave whose amplitude was modulated by a Gaussian, and the length of the pulse was 10 periods. The pulse was reflected by the reflector and received by the transducer after a certain amount of time. To compare the received signal with the transmitted signal we normalized the amplitudes and applied a 180 degrees phase shift to account for attenuation and the phase shift due to reflection, respectively. Finally, by shifting the position of the received signal along the time axis such that the transmitted and received signals overlap, we determine the time-of-flight of the pulse. In Figure 3 the manipulated reflected signal is illustrated with black dots and its envelope is plotted with a black solid curve. The center frequency f_c of the system was set at 5.208MHz and the sampling frequency was $4\times f_c$. As a result, there are roughly 4 data points in one period.

The envelopes of the signals reflected from different distances between the transducer and the reflector are plotted together in Figure 3 (right). As expected, a linear increase of the distance results in equally spaced received signals. On the other hand, the amplitude of the received

signal, which is represented by the amplitude of the envelope of the signal, is proportional to the sound pressure or square root of the sound power. As the wave propagates, the energy should decrease. However, as we can see in the figure, the amplitude firstly increases and then decreases when the reflector is moved further away from the transducer. This is because of the focus of each element on the direction perpendicular to the imaging surface for which we need to correct when measuring the attenuation in a sample.

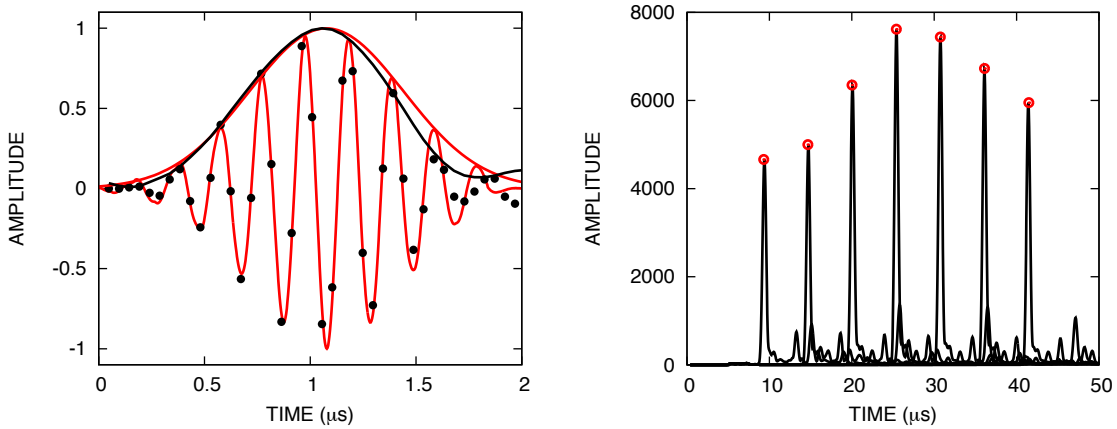

Figure 3 – Left: Comparison between the transmitted signal from the ultrasound transducer (red) and the received signal (black). Right: Envelopes of the received signals reflected from different distances (equally separated from 4mm to 28mm). The red circles label the peak of each envelope.

Calibration for Cornstarch Suspensions

To correct for signal attenuation we can use time gain compensation (TGC), so that signals that arrive later are amplified more. To set TGC properly, the attenuation needs to be measured. We employed two methods.

First, we used a similar method as mentioned in the previous section: we moved the position of a flat reflector in the sample and measured the amplitude of the reflected signal. In this case the sample was a density matched cornstarch suspension with a packing fraction of 45% by weight. The TGC was set to a constant because we are interested in the decay. The original amplitudes of the signals reflected from different depths are shown in Figure 4 (left) with the red data points. After applying the amplitude correction discussed in the previous section, we observe an exponential decay. The slope of the line represents the attenuation factor of the sample. If we adjust the TGC according to the decay rate measured, this will balance the amplification and equal out the signal amplitudes, so in the reconstructed images the brightness will be uniform (limited by the capability of the amplifiers).

Second, we measured the signal amplitude reflected at different depths in a density matched cornstarch suspension with a packing fraction of 40%. In this case there was no flat reflector in the sample, and the signals were reflected inside the suspension by air bubbles, which act as strong scatterers. The averaged signal amplitude (along the transverse direction of the beam) is plotted in Figure 4 (right). The TGC was set constant for each individual measurement, but successively stepped from 100 to 900 (the adjustable range is 0 to 1023). When normalized by their amplifications, all signals show an initial exponential decay before the noise floor is

reached at larger depth. This crossover is seen to depend on the amplification, i.e. on the TGC setting.

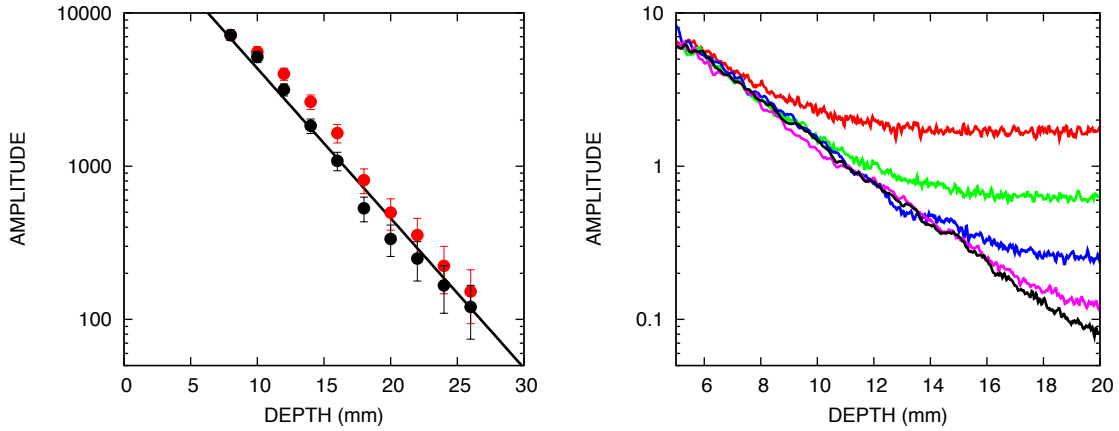

Figure 4 – Left: Attenuation of the reflected signal in 45% degassed cornstarch suspension before (red) and after (black) the amplitude correction. Right: Amplitude of signals in 40% non-degassed cornstarch suspension at different amplifications. Color indicates TGC: red-100, green-300, blue-500, pink-700 and black-900. The amplitudes were normalized by TGC = 1.

Calibration of Particle Image Velocimetry using Gelatin Samples

In order to measure the propagation of the jamming front and the flow around the jamming front, we need to use particle image velocimetry (PIV) to the reconstructed ultrasound images. To check whether the velocities of uniformly distributed small scatters can be captured by the ultrasound correctly, we measured the velocity field of a layer of particles embedded in a sheared gelatin sample. We used a gelatin sample because it is transparent and thus allows us to compare the ultrasound results to standard PIV obtained with a high-speed camera. In the experiment, the sample was imaged simultaneously with the ultrasound and a high-speed camera.

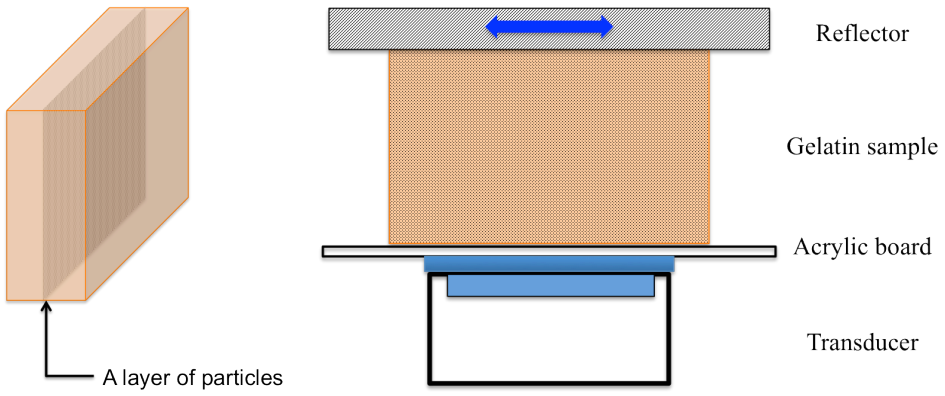

Figure 5 – Left: A schematic illustration of the gelatin sample embedded with a layer of scattering particles. Right: A schematic illustration of the experimental setup. The blue double sided arrow in the reflector means that the reflector was moved horizontally to shear the sample.

As illustrated in Figure 5 (left), the gelatin was a rectangular sample made of 10% (w/w) gelatin solution in water. A number of spherical particles were uniformly distributed in the middle of the

sample, forming a thin sheet of scatters. The gelatin sample deforms elastically (it does not flow), so the scatters move proportional to the applied shear. The experimental setup is shown in Figure 5 (right). The gelatin sample was placed with the particle layer vertical on a 5/64 inch thick acrylic support and sheared by a reflector on the top. A transducer was placed below the acrylic support, and the imaging plane of the transducer was aligned with the layer of particles in the sample. A high-speed camera was positioned perpendicular to the layer of particles. The resolution of the images was 6.56×10^{-5} m/pixel, high enough to resolve every individual particle.

As shown in Figure 6 (left), we applied PIV analysis on both the camera (top) and ultrasound (bottom) images to obtain the velocity field of the sheared sample. The image is divided into square elements and the velocity of each element is calculated through a cross-correlation algorithm between two subsequent frames. The calculated velocities are represented by green arrows. For clarity, we only show a part of the sample here. For the whole sample, the elements at the bottom have zero horizontal velocity and those on the top moves with the velocity of the reflector. As expected for an elastic solid, the horizontal velocities increase linearly with the height.

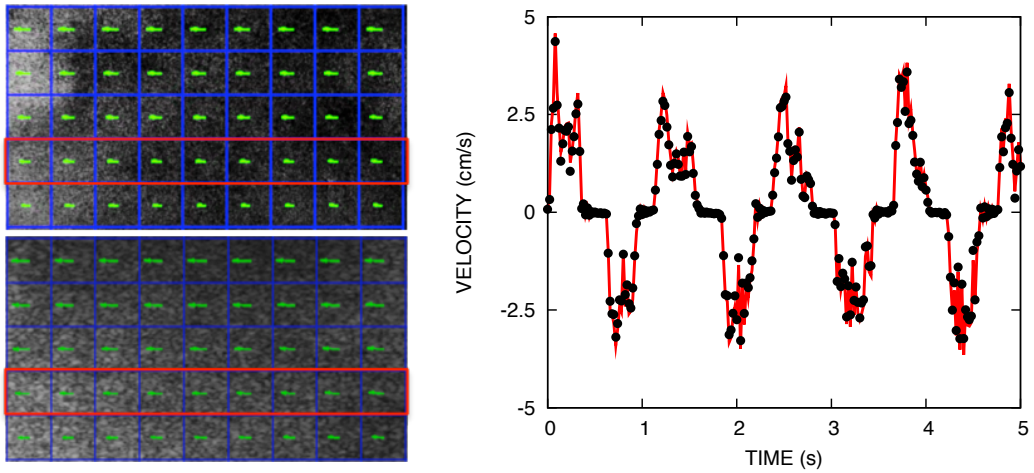

Figure 6 – Left: Part of the flow field of a sheared gelatin sample imaged by a camera (top) and the same sample imaged by the ultrasound (bottom). Right: Velocity averaged over a horizontal line (labeled with red boxes on the left) at a single vertical position as a function of time, measured by the camera (red line) and the ultrasound (black points).

Figure 6 (right) shows an excellent agreement of the ultrasound results with the direct optical measurements. In this figure, we plot the average velocity as a function of time at a given height for both the camera (red) and the ultrasound (black). The sample was sheared in a quasi-random manner with significant amount of small-scale variation in the applied shear rate, all of which is captured well by the ultrasound measurement.

We tested spherical scatters with two different diameters, $d = 2\lambda$ and $d = 0.3\lambda$, where λ is the wavelength of the sound wave. The smaller particles test the behavior of our PIV method for cornstarch particles, which are similar in size ($d \sim 0.1\lambda$). Theoretically, the resolution of an imaging system is limited by its wavelength, and only objects with a length scale greater than the wavelength can be resolved. This is certainly true here too: we can tell the positions of individual particles in an ultrasound image when $d = 2\lambda$, but only see a speckle pattern when $d = 0.3\lambda$.

However, it is not necessary to know the actual position of each individual particle to measure the velocity field because a displacement of particles results in the same displacement of the speckle pattern, which we confirmed with our calibrations. The velocity measurements match very well in both experiments ($d = 2\lambda$ and $d = 0.3\lambda$), so although we cannot locate the particles when they are smaller than a wavelength (e.g., cornstarch particles) we can still accurately measure the velocity field.

Preliminary Data

Speed of Sound

As a first measurement we obtained the speed of sound in dense suspensions at different packing fractions Φ. As test suspension we used cornstarch particles in water, and density matched the particles with a CsCl water solution (density of 1.59g/cm^3). The setup was was te same as shown in Figure 1 (right). From the known position of the reflector and the measured travelling time of the sound pulse the speed of sound was obtained for a range of suspensions of different packing fraction. The experimental result is shown in Figure 7, along with theoretical predictions illustrated by the red curves. In the regime that we work in, where the wavelength is much larger than the particle diameter, the speed of sound c is predicted by an effective-medium model

$$c = \sqrt{\beta_{eff}/\rho_{eff}} = \left[\phi\rho_s + (1-\phi)\rho_f\left(\frac{\phi}{\beta_s} + \frac{1-\phi}{\beta_f}\right)\right]^{-1/2}. \qquad (1)$$

Here β is the elastic modulus, ρ represents the density, and the subscripts s and f refer to the solid (particles) and fluid subphases, respectively. For our density matched case $\rho_s = \rho_f = 1.59$g/cm^3, and B_f can be obtained from c at $\Phi = 0$. The remaining fitting parameter is B_s.

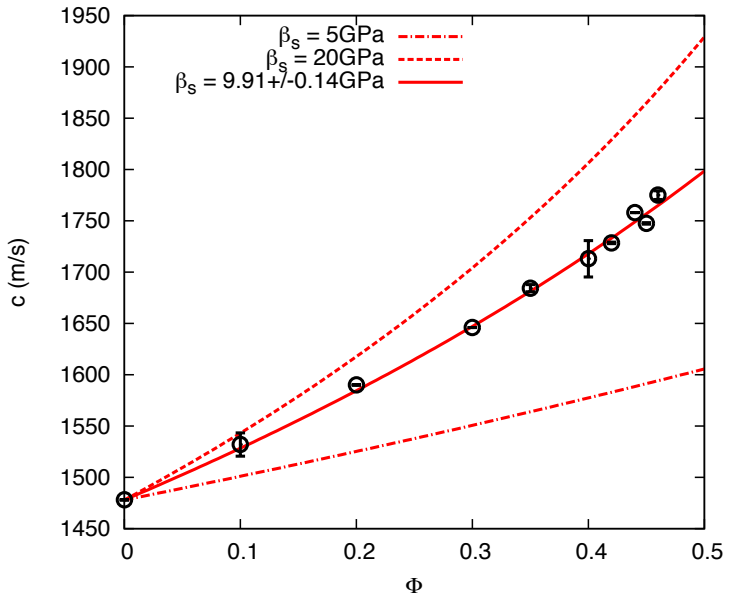

Figure 7 – Speed of sound c in density matched cornstarch suspensions at different packing fractions Φ. The solid red line is a fitting of the data with Equation XX and the dashed red lines are predictions of the trend at two other particle moduli β_s.

For granular materials like cornstarch very few reference data exist currently. Fitting our data to Equation 1 we obtain that β_s = 9.9±0.2GPa. This agrees with the values available from ultrasound measurements of similar suspensions, and also with values obtained from atomic force microscopy indentation measurements, where we found β_s ~7±3GPa. For comparison we show in the same plot curves for β_s = 5GPa and 20GPa.

The speed of sound measurement is key to reconstructing ultrasound images because, as described earlier, the ultrasound can measure longitudinal distance correctly only when c is known. The same method also provides a straightforward way to measure the elastic modulus of the particle subphase in a suspension. Importantly, measurements of the speed of sound can be used to track changes of the packing fraction Φ. We are currently working on using other acoustic properties of the material such as its acoustic impedance and attenuation to determine the packing fractions. Measuring these properties dynamically is more challenging than measuring the speed of sound; however, the attenuation factor is more sensitive to changes in Φ than the speed of sound, and thus have the potential to provide better accuracy.

Effect of Trapped Air Bubbles

We noticed that the brightness of the cornstarch suspension decreased when compressed quickly, as shown in Figure 8 (left). The experimental setup was similar to the schematic plot in Figure 1 (right), with the reflector attached to the Instron so that the force applied on the reflector could be measured simultaneously with the ultrasound imaging. The reflector (which appears as a bright horizontal feature in the images) was pushed downward. The color in the images represents the amplitude of the reflected signal, with red corresponding to strong reflection and blue representing the background. Between image (a) and (b) the reflector moved closer to the bottom of the container but the pressure did not change much. In (b) we observed a stronger signal reflected from the reflector and slightly weaker reflections in the region between the reflector and the bottom compared to (a). In (c), the suspension has solidified under the applied stress ($2P_0$ as measured by the Instron), and it is very clear that the region became much darker than (b) and that the reflector almost disappeared. After (c), the downward motion was stopped, after which the brightness recovered and the reflector showed up again, see (d).

Figure 8 (right) shows the averaged signal amplitudes as function of depth for different applied stress by the Instron. The peak at about 14mm is the reflection from the wall of the syringe opposite to the transducer. From this plot we deduce two aspects: (1) the amplitude of the signal reflected from the sample (the decay part) decreased with pressure, and (2) the amplitude of the signal reflected from the wall increased with pressure. This means that the decrease of brightness is not an effect of increasing attenuation, because in that case we would not see a stronger reflection from the opposite wall. Instead, it is caused by a decrease of reflections from the scatterers in the suspension.

As illustrated in the inset of Figure 8 (right), we found that when the suspension was degassed, it became acoustically transparent, and only a very small amount of reflection was observed. Therefore, the scatterers in the suspension that reflect most of the signal are tiny air bubbles. This is confirmed by the response to changes in pressure of the system: with increasing pressure the scattering bubbles decrease in size, so they are less effective in scattering the ultrasound. As a result, the suspension becomes more transparent (and thus darker in the images), and produces a stronger signal from the reflector due to decreased attenuation.

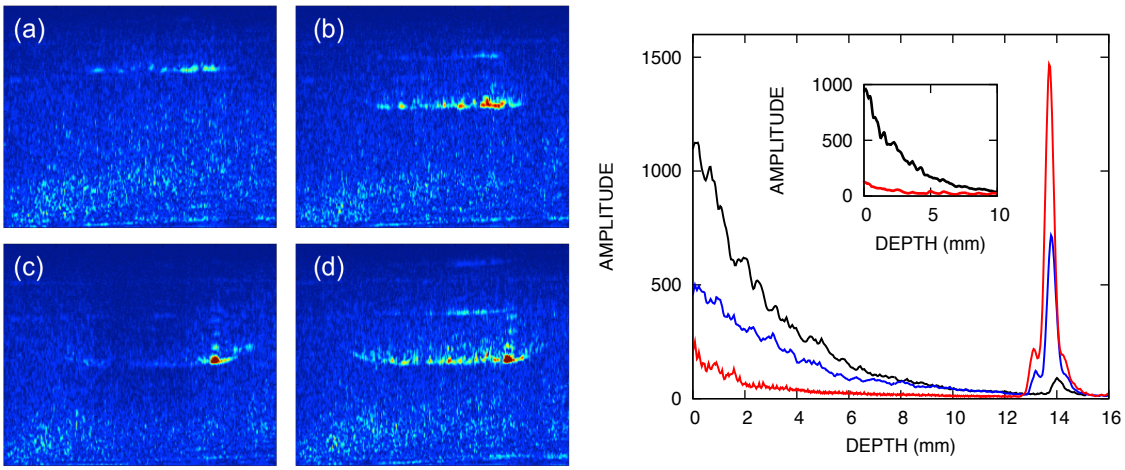

Figure 8 – Left: Change of brightness of the reflected signal in cornstarch suspension when compressed. Right: The amplitude of reflected signals in cornstarch suspension at different applied stress: black-$1P_0$, blue-$4P_0$ and red-$7P_0$, where P_0 is a stress level corresponding to atmospheric pressure (1 bar). Inset: The amplitude of reflected signals in degassed (red) and non-degassed (black) cornstarch suspensions.

These findings do, however, not completely explain the compressing experiment shown in Figure 8 (left). Clearly, in Figure 8 (c) the intensity of the signal reflected from the reflector decreased dramatically, where we would expect an increase if the suspension had undergone a simple compression. We suspect that there is a second effect responsible for this, such as, for example, solidification of the material, but this is still work in progress.

Transient Response due to Impact

A major goal was to use the ultrasound to extract the velocity field inside a cornstarch suspension as it evolves under impact. To achieve this there are several requirements: (1) a high enough frame rate to observe the growth of the front, which typically moves an order of magnitude faster than the pusher; (2) a reasonable penetration depth in the suspension, at least several centimeters; (3) reliable tracer particles that reflect the real motion of the suspension. Currently, the frame rate we can reach reliably with the Verasonic system is 5000 frames per second, which is high enough to see the propagation of the front (we are in the process of increasing this to 10,000 frames per second). We have increased the penetration depth dramatically by degassing the suspension. As described above, we have confirmed that the ultrasound system can measure accurately the velocity field of uniformly distributed scatterers. Furthermore, from our experiments described in section just above, we know that the most effective scatters in the suspension are air bubbles. Consequently, we can measure the flow field effectively by tracking the motion of air bubbles in it.

We have tested two ways of introducing air bubbles to a degassed cornstarch suspension: (1) mixing it with non-degassed suspension; (2) briefly but sharply tapping the surface of the suspension. The former method mostly introduces bubbles smaller than the ultrasound wavelength, and therefore it generates a speckle pattern. The latter method, mostly introduces big bubbles that can be located individually in the reconstructed images. Both methods work for tracking the flow, and we have checked with a rheometer that the existence of (small amounts of)

air bubbles in a cornstarch suspension does not change its rheological behavior at high shear rates.

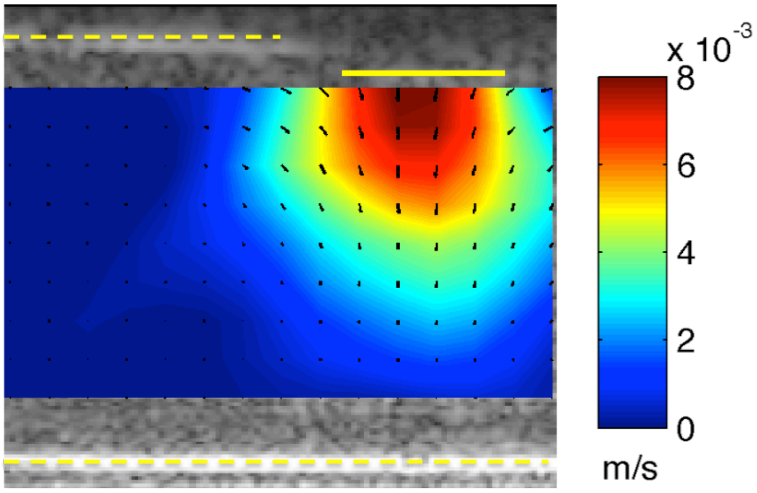

Figure 9 – Flow field in a density matched cornstarch suspension under vertical impact. The color code represents the magnitude of the vertical velocity. The two horizontal dashed yellow lines denote the fluid surface and the bottom of the container, respectively. The solid yellow bar indicates the position of the pusher (reflector).

One frame from the impact experiment is shown in Figure 9 as an example. In the figure the dashed yellow line at the bottom indicates the bottom of the container, and the dashed line on the top indicates the initial position of the surface. The solid yellow bar represents the bottom surface of the pusher, showing both its position and its width. The black arrows are obtained from the PIV analysis and represent the local flow velocity (magnitude and direction) in the suspension. The color represents the magnitude of the vertical component of the local velocity, ranging from 0 mm/s (blue, stationary background) to 8 mm/s, the velocity of the pusher (red).

From velocity field like this one, we can extract the shape of the jammed region and track its propagating front as it evolves in response to impact at the free surface. Currently, no detailed information about this evolution is available for fully three-dimensional systems (we have been able to perform x-ray imaging at 30fps, but this is far too slow to capture the transient behavior). The only PIV tracking performed so far has been on two-dimensional layers of suspension (performed by postdoc Ivo Peters in our group). The ultrasound imaging experiments therefore will provide a firt direct test of whether there are any differences between the two- and three-dimensional situations. Graduate student Endao Han and postdoc Ivo Peters are in the process of completing these measurements. A manuscript is in preparation.

Shear Profile

We have also obtained preliminary results using the shear setup described earlier. The ultimate goal of this experiment is to measure the transient shear profile inside the bulk of a dense suspension in response to an impulsive start of the inner cylinder (see Fig. 10), and then relate this to the applied torque. This is the equivalent to tracking an impact induced solidification front, as just discussed above, but now the front is generated by shear.

A single measurement will measure the velocity profile in a single horizontal plane at a vertical position z. By using a common, simultaneous trigger signal for the rheometer and the ultrasound system, this measurement can be repeated and averaged to increase the signal-to-noise ratio. Then, by measuring the transient response at different z-positions, we are able to map out the 3-dimensional transient profile. We have not quite completed this type of analysis yet, but we expect the result be independent of z, given that we are far enough away from the bottom of the shear cell.

In addition, postdoc Ivo Peters has performed measurements of the steady-state shear profiles for moderately concentrated suspensions (packing fractions up to ~ 30% in volume), where we do not get into a jammed state. These experiments will serve both as a test to determine the capabilities of the ultrasound system and the design of the setup to determine the internal velocities and as a reference for comparison with transient responses. We started the experiment with pure water, and then added cornstarch to the liquid to increase the packing fraction. We measured velocities using PIV, the same way as described above for the impact experiment.

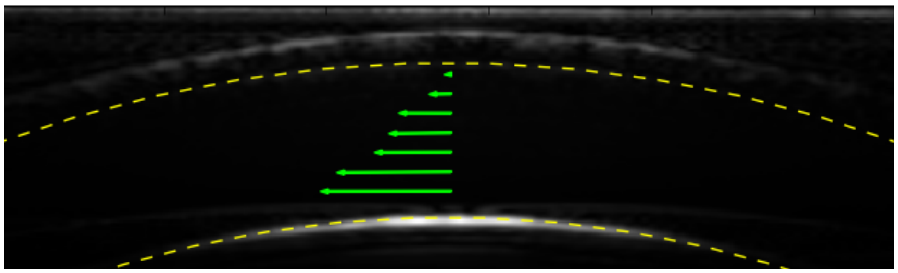

Figure 10 – Ultrasound image of the Couette-geometry, with the measured velocity profile (green arrows). The yellow dashed lines indicate the cylinder walls.

Figure 10 shows an example of the measured velocity in the suspension. The bright curved line at the bottom of the image represents the position of the inner cylinder. The exact location of the outer cylinder is less clearly visible: the bright curved line at the top of the image is an artifact due to internal reflections – the edge of the outer cylinder is just below it and can be seen as a fainter curved line. For clarity, we indicate the cylinder walls with dashed yellow lines. As expected, the velocity is the highest near the inner (rotating) cylinder and drops to zero towards the outer (stationary) cylinder.

A paper on the transient shear response is in the early stages of preparation.